Journal of Power Sources 223 (2013) 125–128

Contents lists available at SciVerse ScienceDirect

Journal of Power Sources

journal homepage: www.elsevier.com/locate/jpowsour

Short communication

Enhanced glucose electrooxidation at a binary catalyst of manganese and nickel oxides modified glassy carbon electrode

S.M. El-Refaei, M.M. Saleh, M.I. Awad*

Department of Chemistry, Faculty of Science, Cairo University, Cairo 12613, Egypt

HIGHLIGHTS

- ► NiO_x/MnO_x/GC electrode significantly catalyzes glucose oxidation.
- ► Order of deposition of oxides is a crucial in the electrocatalytic activity.
- ► A synergistic enhancement effect between the two oxides is concluded.

ARTICLE INFO

Article history:
Received 21 May 2012
Received in revised form
31 July 2012
Accepted 22 August 2012
Available online 18 September 2012

Keywords:
Glucose
Manganese oxide
Nickel oxide
Fuel cell
Nano

ABSTRACT

A novel binary electrocatalyst fabricated from manganese and nickel oxides nanoparticles (MnO_x and NiO_x), prepared by electrodeposition, is proposed as an anode for an amplified electrochemical oxidation of glucose in NaOH solutions. Cyclic voltammetry and scanning electron microscopy images were used to characterize these electrocatalysts. It has been found that the electrocatalytic activity critically depends on the order of the deposition of the two oxides. The NiO_x/MnO_x/GC electrode (MnO_x deposited first) showed a superior electrocatalytic activity towards glucose oxidation compared to NiO_x/GC, MnO_x/GC or MnO_x/NiO_x/GC electrodes (NiO_x deposited first). The extraordinary activity obtained at the NiO_x/MnO_x/GC electrode is attributed to the compilation of the better adsorption of glucose molecules on the MnO_x sites and the increase of conductivity of the NiO_x due to the increase of Ni^{3+} content. The results lead us to conclude that there is a synergism between the two oxides towards the electrooxidation of glucose.

1. Introduction

Electrocatalytic oxidation of glucose has gained much attention during the last few decades due to its importance as an enzymeless detection tool for glucose in blood and also as a potential fuel in biofuel cells [1–4]. Many attempts have been introduced to develop efficient electrocatalysts for glucose oxidation. Earlier works have focused on the use of noble metal-based electrocatalysts that include Pt [5–7] and Au [4,8–11]. Recently main attempts have been made to use large numbers of transition metal oxides, including both bulk and nanostructures-based electrodes, such as NiO_x [12], FeOOH [13], CuO [14], MnO_2 [15], RuO_2 [16], Cu_2O and Co_3O_4 [17,18]. Among these oxides NiO_x and MnO_x are attractive electrocatalysts for glucose oxidation. It is also well-known that nickel and nickel hydroxide exhibit excellent electrocatalytic performance in alkaline medium [19–21].

On the other hand, it has been found that MnO_x deposited on Pt electrode enhanced glucose oxidation that was rationalized as a combined effect of two factors; enhancing glucose adsorption and mediating the electrooxidation of glucose by MnO_x. Thus, MnO_x acting not only as a simple electron sink but also as a catalyst i.e., catalytic mediator [22].

To the best of our knowledge the combined use of NiO_x and MnO_x as a bicatalyst to exploit their combined characteristics for better enhancement of glucose electrooxidation has not been reported. In the present article a novel binary electrocatalyst composed of nanoparticles of NiO_x/MnO_x modified GC electrode is fabricated electrochemically and characterized by SEM and cyclic voltammetry in order to assess its performance for glucose electrooxidation.

2. Experimental

All chemicals used in this work were of analytical grade and were purchased from Merck, Sigma Aldrich and they were used as

* Corresponding author. Tel.: +20 2 3567 6603; fax: +20 2 3567 7556.
E-mail addresses: mahmoudsaleh90@yahoo.com (M.M. Saleh), mawad70@yahoo.com (M.I. Awad).

0378-7753/$ – see front matter © 2012 Elsevier B.V. All rights reserved.
http://dx.doi.org/10.1016/j.jpowsour.2012.08.098

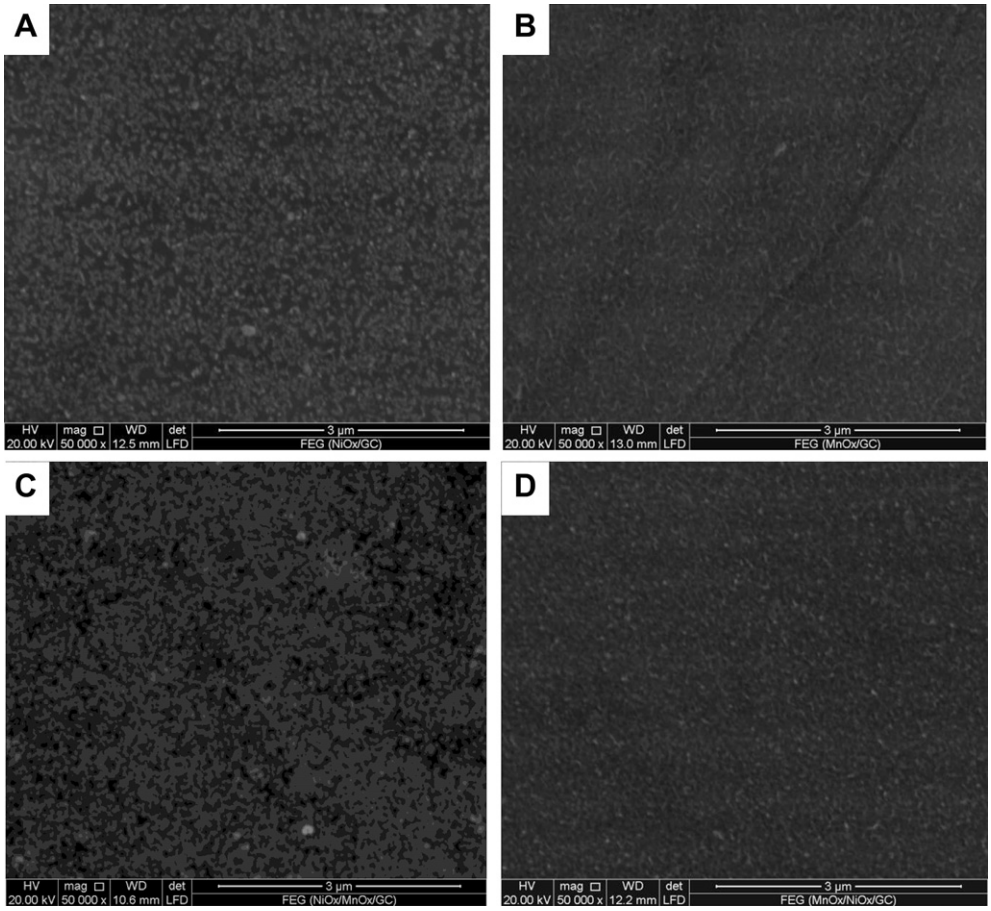

Fig. 1. FE-SEM images of (A) NiO_x/GC, (B) MnO_x/GC, (C) NiO_x/MnO_x/GC and (D) MnO_x/NiO_x/GC.

received without further purification. All solutions were prepared using second distilled water.

Electrochemical characterizations were performed using an EG&G potentiostat (model 273A) operated with E-Chem 270 software. An electrochemical cell with a three-electrode configuration was used in this study. A platinum spiral wire and an Ag/AgCl/KCl(sat.) were employed as counter and reference electrodes, respectively. The working electrode was glassy carbon ($d = 3.0$ mm). It was cleaned by mechanical polishing with aqueous slurries of successively finer alumina powder (down to 0.06 μm) then washed thoroughly with second distilled water.

The electrode modification with nano-NiO_x was achieved in two sequential steps. The first involved the electrodeposition of metallic nickel on the working electrode (i.e., GC) from an aqueous solution of 0.1 M acetate buffer solution (ABS, pH = 4.0) containing 1 mM $Ni(NO_3)_2 \cdot 6H_2O$ by a constant potential electrolysis at −1 V vs. Ag/AgCl/KCl(sat.) for 6 min. Next, the metallic Ni was passivated (oxidized) in 0.1 M phosphate buffer solution (PBS, pH = 7) by cycling the potential between −0.5 and 1 V vs. Ag/AgCl/KCl(sat.) for 10 cycles at a scan rate 200 mV s^{-1} [23,24]. Modification with MnO_x was achieved by cycling potential from 0 to 0.4 V vs. Ag/AgCl/KCl(sat.) in 0.1 M Na_2SO_4 containing 0.1 M $Mn(CH_3COO_2)_2 \cdot 5H_2O$ for 60 cycles, then activation for 5 cycles in 0.5 M NaOH solution in the potential range −0.2–0.6 V [23]. The sequence of the deposition of the two oxides, i.e., NiO_x is deposited first and then MnO_x or vice versa was achieved keeping the number of the cycles or times of the deposition of both catalysts the same. SEM images were taken using field emission scanning electron microscope, FE-SEM (FEI, QUANTA FEG 250).

3. Results and discussion

3.1. Morphological and electrochemical characterizations

The morphological characterization of the modified electrodes is disclosed by SEM imaging and shown in Fig. 1. Image A shows the typical SEM micrograph of NiO_x/GC electrode. It reveals that the NiO_x is deposited as nanoparticles in a uniform distribution with an average particle size about 90–100 nm. Fig. 2 (B) shows SEM

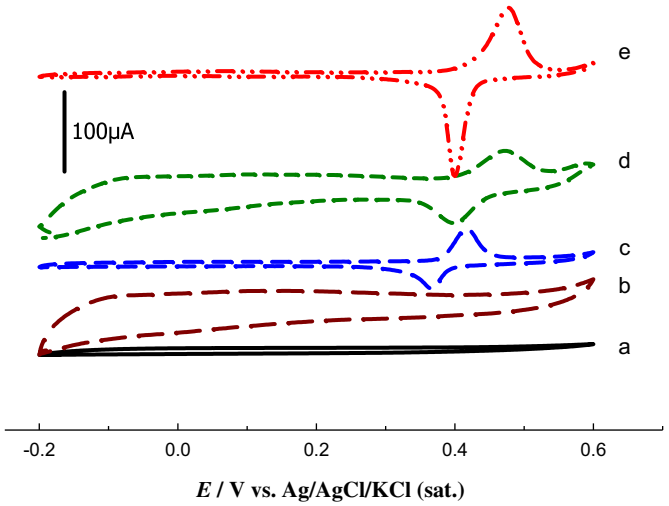

Fig. 2. CVs obtained at: (a) bare GC, (b) MnO_x/GC (c) NiO_x/GC, (d) NiO_x/MnO_x/GC and (e) MnO_x/NiO_x/GC in 0.5 M NaOH solution at a scan rate of 100 mV s^{-1}.

micrograph of MnO_x/GC sample. As can be seen MnO_x is not heavily deposited as much as NiO_x (image A). In image C (NiO_x/MnO_x/GC sample, MnO_x deposited first), NiO_x is extensively deposited as compared with image A. It seems also that NiO_x partially cover the previously deposited MnO_x. In image D (MnO_x/NiO_x/GC sample, NiO_x deposited first) in which MnO_x is deposited on NiO_x/GC the microstructure is not significantly different than the image of deposition of MnO_x directly on bare GC (image B).

Fig. 2 compares CVs of the (a) bare and (b–e) modified GC electrodes in 0.5 NaOH solutions. At bare GC (curve a) and MnO_x/GC (curve b) electrodes the voltammetric behaviours are featureless. Only the charging current significantly increases at the latter electrode as a characteristic feature of the manganese oxide modified electrodes [25]. At the NiO_x/GC (curve c) electrode the well-defined redox waves of the surface confined Ni(II)/Ni(III) is observed; the conversion is represented in acid medium by a proton diffusion in which β-NiOOH is likely formed (Eq. (1)), and by solvent mechanism in alkaline medium in which γ-NiOOH is formed through the diffusion of OH^- (Eq. (2)) [23,24].

$$Ni(OH)_2 \leftrightarrow NiOOH + H^+ + e^- \quad (1)$$

$$Ni(OH)_2 + OH^- \leftrightarrow NiOOH + H_2O + e^- \quad (2)$$

It has been reported that β-NiOOH phase enhances glucose oxidation reaction [26]. The deposition of NiO_x on the MnO_x/GC (NiO_x/MnO_x/GC, curve e) is characterized by marked enhancement in the Ni(II)/Ni(III) couple, especially the cathodic peak, as compared with the NiO_x/GC electrode (curve c). This may be attributed to the increase of the Ni^{3+} content by doping the NiO_x by MnO_x (Eqs. (3) and (4)) which can convert some of the Ni^{2+} to Ni^{3+} resulting in an increase in the conductivity of the former. This may proceed according to the following reactions; (*cf* Section 3.2)

$$Mn(IV) \rightarrow Mn(V) \quad (3)$$

$$Mn(V) + Ni^{2+} \rightarrow Ni^{3+} + Mn(IV) \quad (4)$$

It is noteworthy to mention that the charging current in this case significantly decreases upon the deposition of the NiO_x on the MnO_x/GC electrode, almost the response obtained at NiO_x/GC (curve c) in the potential range −0.2–0.3 V is restored after the deposition of NiO_x onto MnO_x/GC. This is certainly due to the deposition of NiO_x onto the previously deposited MnO_x.

Interestingly Ni(II)/Ni(III) couple significantly decreases when the order of the deposition is reversed, i.e., when MnO_x is deposited onto NiO_x/GC (MnO_x/NiO_x/GC, curve d). This points to the partial deposition of MnO_x on the previously deposited NiOx.

3.2. Electrocatalytic oxidation of glucose at the modified electrodes

Fig. 3 shows CVs of the glucose (20 mM) oxidation at (a) bare and modified GC electrodes (b-e) in 0.5 NaOH solutions, (same notations as in Fig. 2 is used). The oxidation of glucose at GC (curve a) is not feasible indicating the inertness of the GCE towards glucose oxidation under the present conditions. At the MnO_x/GC electrode (curve b) the CV is also featureless as in the absence of glucose. In contrast, the oxidation of glucose at the GC/NiO_x electrode (curve c) is markedly enhanced; it occurs at a lower positive potential, associated with increasing the anodic peak current and diminishing the cathodic peak current resembling the behaviour of a catalytic process. The electrocatalytic oxidation of glucose occurs not only in the forward scan but also in the backward scan [21,27]. Glucose molecules adsorbed on the surface are oxidized at higher potentials parallel to the oxidation

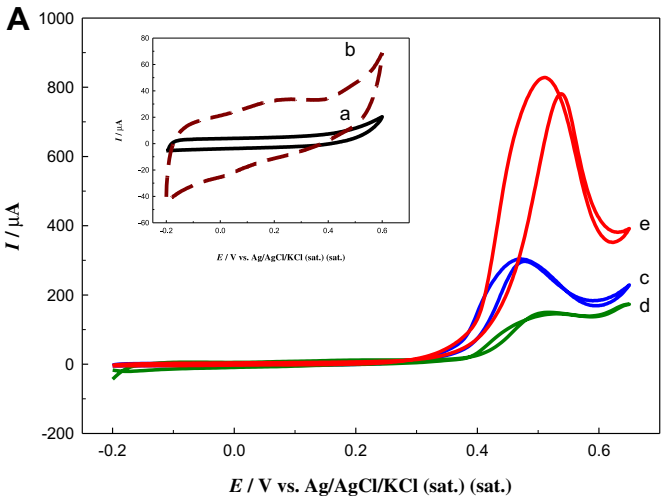

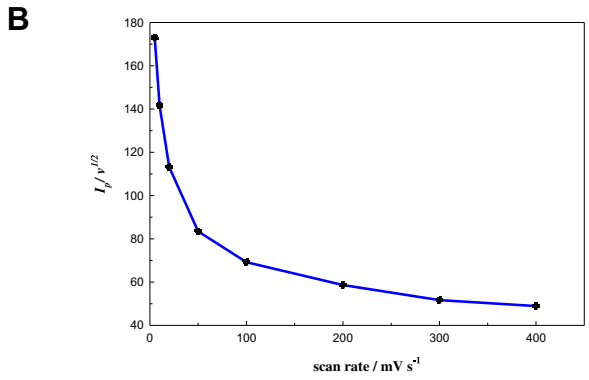

Fig. 3. A. CVs response obtained at (a) GC, (b) MnO_x/GC, (c) NiO_x/GC, (d) NiO_x/MnO_x/GC, and (e) MnO_x/NiO_x/GC electrodes in 0.5 NaOH solution containing 20 mM glucose at a scan rate of 100 mV s^{-1}. B. Variation of $I_p/\nu^{1/2}$ with ν for glucose electrooxidation obtained at NiO_x/MnO_x/GC electrode in 0.5 M NaOH solution containing 20 mM glucose.

of Ni(II) to Ni(III) species. The later process has the consequence of decreasing the number of sites for glucose adsorption, along with the poisoning effect of the products or intermediates of the reaction, and consequently the decrease in the overall rate of the glucose oxidation. Thus, the anodic current passes through a maximum as the potential is anodically swept. In the reverse half cycle, the oxidation continues, and its corresponding current goes through a maximum due to the regeneration of active sites for the adsorption of glucose as a result of the removal of adsorbed intermediates and products. The glucose oxidation at MnO_x/NiO_x/GC and NiO_x/MnO_x/GC electrodes in 0.5 M NaOH is shown as curves d and e, respectively. It is obvious that the order of the deposition of the nano-MnO_x and NiO_x dramatically affects the performance of the binary catalyst. When the MnO_x/NiO_x/GC is used (NiO_x is deposited first) (curve d), the activity significantly decreases. The highest response is obtained on the NiO_x/MnO_x/GC electrode, i.e. when MnO_x is firstly deposited followed by the electrodeposition of NiO_x. The larger response at the binary catalyst NiO_x/MnO_x/GC (curve e) in comparison with NiO_x/GC (curve c) electrode may be the result of two factors; firstly, glucose is expected to be adsorbed quite easily on MnO_x due to the possibility of hydrogen bond formation using the multiple hydroxyl groups present in the molecule [28]. Thus the accessibility of glucose at the electrode surface increases. In addition MnO_x plays a significant role in freeing the NiO_x from any poisoning intermediate

[29,30]. Then the glucose oxidation is mediated by Ni(II)/Ni(III) couple producing gluconolactone as oxidation product [31,32] as represented by Eqs.(5) and (6).

$$\mathrm{Ni(II)} \rightarrow \mathrm{Ni(III)} + \mathrm{e}^- \quad (5)$$

$$\mathrm{Ni(III)} + \mathrm{glucose} \rightarrow \mathrm{gluconolactone} + \mathrm{Ni(II)} \quad (6)$$

It has been reported that carbohydrate oxidation is electrocatalyzed at MnO_x modified electrodes, and the source of catalysis was explained on the basis of EC mechanism. The formation of Mn(V) was proved according to the following reaction Mn(IV) → Mn(V) + e [29,30]. Mn(V) was considered as a strong oxidant that can oxidize glucose molecules and converted back to MnO_2. Indeed the +5 oxidation state is considered to be an important intermediate in the mechanism of redox process involving different Mn compounds [29,30]. Yet from the above consideration Ni^{2+} can be oxidized to Ni^{3+} by the strong oxidant Mn(V). Increasing the concentration of Ni^{3+} in the matrix can increase the conductivity of the matrix and enhance the glucose oxidation via (Eq. (6)). This could increase the current peak of the redox couple Ni^{2+}/Ni^{3+}. It is noteworthy to mention that the amount of the deposited Ni, as estimated from the deposition curves, in the case of single electrode NiO_x/GC and binary electrode NiO_x/MnO_x/GC to equal 7.8 and 10 μg, respectively. The amount of the deposited nickel in the case of binary electrode is higher than single electrode, but this increase in the amount of the deposited nickel can't account for the difference in the current density between the single and binary electrode.

On the other hand at MnO_x/NiO_x/GC electrode (curve d) the response for glucose significantly decreases. According to (Fig. 2e) the couple Ni^{2+}/Ni^{3+} decreases upon the deposition of MnO_x on the GC/NiO_x indicating the partial coverage of the previously deposited NiO_x. It could be concluded that the exposition of the two oxides is essential for the electrocatalytic oxidation of glucose. At the NiO_x/MnO_x/GC electrode the current is 2.5 and 7 times higher than that obtained at NiO_x/GC and NiO_x/MnO_x/GC electrodes, respectively.

Fig. 3B shows the variation of the reaction function ($I_p/\nu^{1/2}$) with ν obtained at the NiO_x/MnO_x/GC electrode. As can be seen at scan rate higher than 50 mV s^{-1}, $I_p/\nu^{1/2}$ does not change significantly with scan rate, which is a characteristic feature of catalytic reactions [33]. It becomes clear that NiO_x/MnO_x/GC electrode significantly enhances the glucose electrooxidation via a dual role exerted by the mixed oxides; MnO_x enhances the adsorption of glucose and then the mediation by the second oxide (NiO_x) in an EC mechanism as represented by Eqs. (5) and (6) and confirmed by the $I_p/\nu^{1/2}$–ν relation (Fig. 3B). The stability of the proposed catalysts towards glucose oxidation was investigated by recording current–time curves for 3 h at a constant potential (520 mV), and it was found that the stability of the electrode is satisfactory; it was found that the current almost keeps constant over the studied time range.

4. Conclusions

Nickel and manganese oxides binary catalysts were deposited electrochemically in a consecutive manner on a glassy carbon electrode, and tested for the electrooxidation of glucose in alkaline media. It showed an excellent enlarging of the current corresponding to glucose oxidation at a reasonable overpotential compared to nickel oxide alone. The order of the deposition of oxides played a crucial role in the electrocatalytic activity of the modified electrodes. $I_p/\nu^{1/2}$ decreases with increasing ν, which is a characteristic feature of a catalytic process.

References

[1] Y. Liu, H. Teng, H. Hou, T. You, Biosensors and Bioelectronics 24 (2009) 3329.
[2] A. Sun, J. Zheng, Q. Sheng, Electrochimica Acta 65 (2012) 64.
[3] F. Mizutani, S. Yabuki, Biosensors and Bioelectronics 12 (1997) 1013.
[4] M. Tominaga, T. Shimazoe, M. Nagashima, I. Taniguchi, Electrochemistry Communications 7 (2005) 189.
[5] S.S. Mahshid, S. Mahshid, A. Dolati, M. Ghorbani, L. Yang, S. Luo, Q. Cai, Electrochimica Acta 58 (2011) 551.
[6] Y. Bai, Y. Sun, C. Sun, Biosensors and Bioelectronics 24 (2008) 579.
[7] J. Lu, S. Lu, D. Wang, M. Yang, Z. Liu, C. Xu, S.P. Jiang, Electrochimica Acta 54 (2009) 5486.
[8] M. Pasta, F. La Mantia, Y. Cui, Electrochimica Acta 55 (2010) 5561.
[9] M. Tominaga, Y. Taema, I. Taniguchi, Journal of Electroanalytical Chemistry 624 (2008) 1.
[10] A.K. Singh, S. Srivastava, J. Srivastava, R. Srivastava, P. Singh, Journal of Molecular Catalysis A: Chemical 278 (2007) 72.
[11] H.-B. Noh, K.-S. Lee, P. Chandra, M.-S. Won, Y.-B. Shim, Electrochimica Acta 61 (2012) 36.
[12] C. Li, Y. Liu, L. Li, Z. Du, S. Xu, M. Zhang, X. Yin, T. Wang, Talanta 77 (2008) 455.
[13] C. Xia, W. Ning, Electrochemistry Communications 12 (2010) 1581.
[14] L.-C. Jiang, W.-D. Zhang, Biosensors and Bioelectronics 25 (2010) 1402.
[15] D. Das, P. Sen, K. Das, Journal of Applied Electrochemistry 36 (2006) 685.
[16] J. Shim, M. Kang, Y. Lee, C. Lee, Microchimica Acta 177 (2012) 211.
[17] L. Zhang, H. Li, Y. Ni, J. Li, K. Liao, G. Zhao, Electrochemistry Communications 11 (2009) 812.
[18] Y. Ding, Y. Wang, L. Su, M. Bellagamba, H. Zhang, Y. Lei, Biosensors and Bioelectronics 26 (2010) 542.
[19] S. Berchmans, H. Gomathi, G. Prabhakara Rao, Sensors and Actuators B: Chemical 50 (1998) 156.
[20] M. Vidotti, C.D. Cerri, R.F. Carvalhal, J.C. Dias, R.K. Mendes, S.I. Córdoba de Torresi, L.T. Kubota, Journal of Electroanalytical Chemistry 636 (2009) 18.
[21] S. Berchmans, H. Gomathi, G.P. Rao, Journal of Electroanalytical Chemistry 394 (1995) 267.
[22] Y.J. Yang, S. Hu, Electrochimica Acta 55 (2010) 3471.
[23] D. Giovanelli, N.S. Lawrence, L. Jiang, T.G.J. Jones, R.G. Compton, Sensors and Actuators B: Chemical 88 (2003) 320.
[24] D. Giovanelli, N.S. Lawrence, S.J. Wilkins, L. Jiang, T.G.J. Jones, R.G. Compton, Talanta 61 (2003) 211.
[25] H. Usui, K. Meabara, K. Nakai, H. Sakaguchi, International Journal of Electrochemical Science 6 (2011) 2235.
[26] M. Jafarian, F. Forouzandeh, I. Danaee, F. Gobal, M. Mahjani, Journal of Solid State Electrochemistry 13 (2009) 1171.
[27] H. Heli, M. Jafarian, M.G. Mahjani, F. Gobal, Electrochimica Acta 49 (2004) 4999.
[28] D. Das, P.K. Sen, K. Das, Journal of Electroanalytical Chemistry 611 (2007) 19.
[29] D. Das, P.K. Sen, K. Das, Electrochimica Acta 54 (2008) 289.
[30] I.-H. Yeo, D.C. Johnson, Journal of Electroanalytical Chemistry 484 (2000) 157.
[31] C. Zhao, C. Shao, M. Li, K. Jiao, Talanta 71 (2007) 1769.
[32] I. Becerik, F. Kadirgan, Electrochimica Acta 37 (1992) 2651.
[33] M.S. El-Deab, Journal of Advanced Research 1 (2010) 87.